Localized Thermal Analysis for Sportswear via Wind Tunnel Testing

Xiaoyi Cai^{®a}, Zixiang Hu^{®b} and Peng Zhou

Department of Mechanical and Aerospace Engineering, The Hong Kong University of Science and Technology, Clear Water Bay, Kowloon, Hong Kong SAR, China

Keywords: Sportswear, Thermal Comfort, Wind Tunnel, Convective Heat Transfer Coefficient, Thermal Insulation.

Abstract:

Thermal comfort of sportswear is critical for optimizing athletic performance and improving safety. However, current research on the convective heat transfer coefficient (h) between fabrics and the air flow remains limited, especially in terms of its local analysis. In this study, a thermal cylinder which simulates human limb was developed to evaluate the fabrics' thermal insulation (I) and h (both local and global values) in the wind tunnel. The wind speed ranged from 2 to 8 m/s, and the stretch ratio (SR) from 1.1 to 2.0. The results show that for both fabrics, the local h reaches a minimum around $\theta = 80^{\circ}-90^{\circ}$, while the local I_{t} peaks near $\theta = 120^{\circ}$. The effects of SR and wind speed on I_{t} and h are also reported. This work offers a practical method for quantifying the heat transfer characteristics of stretched fabrics, providing theoretical guidance for sportswear design and thermal regulation strategies in wind environment.

1 INTRODUCTION

Thermal performance of sportswear is a critical factor influencing both athletes' competitive performance and physiological safety (Domenico et al., 2022). On one hand, effective heat dissipation from the body surface improves thermal comfort, which is important for endurance, concentration, and neuromuscular efficiency during exercise. On the other hand, inadequate thermal regulation can lead to the accumulation of metabolic heat and moisture, increasing the risk of thermal stress, dehydration, and heat-related illnesses (Douzi et al., 2020; Reilly et al., 2006). Therefore, a comprehensive understanding of the thermal performance of sportswear is essential for designing garments and providing guidance for enhancing athletes' competitive performance.

Research on evaluating the thermal performance of sportswear mainly focuses on the thermal insulation (I_t) and evaporative resistance ($R_{\rm et}$). Several researchers have investigated the influence of fabric physical parameters on thermal insulation and evaporative resistance, including factors such as fabric layer and yarn type. A common conclusion from these studies is that thermal insulation tends to increase with increasing fabric thickness and the

volume ratio of air layer. Using heated thermal manikins, Wang et al. (2012; 2016) and Fan et al. (2008) studied the effects of body motion, body regions, and sweat rates on the global evaporative resistance. Similarly, Preet et al. (2018; 2023) explored the body-related factors, including sweat composition and concentration. The impact of varying wind conditions on thermal insulation and evaporative resistance has also been studied (Hu et al., 2016; Cui et al., 2016); however, the maximum wind speed in these works was limited to 1.5 m/s. Research on fabrics' It and Ret under static or low wind speed conditions are listed in Table 1.

In real-world athletic activities such as cycling, wind speeds usually exceed 5 m/s. Under such conditions, convective heat transfer plays a significant role in thermoregulation. Therefore, investigating the convective heat transfer coefficient (h) is of practical significance for competitive sports and recreational sports. Although there have been standardized American Society of Testing Materials (ASTM) test methods for evaluating thermal insulation and evaporative resistance of fabrics (ASTM, 2022; ASTM, 2016), research focusing on convection heat transfer of fabric remain limited, and there is still no international testing standards for the

Researchers	Motivation	Method* Variables		
Tesinova et al., 2022		Commercial instruments	Number of layers	
Özkan et al., 2023	Study the effect of fabric structure or composition	Commercial instruments	Type of yarn	
Kumar et al., 2021		Commercial instruments	Blend rate of fabrics	
Saeed et al., 2022		Commercial instruments	Combination of fabrics	
Noshro. et al., 2024		Commercial instruments	Porosity of fabric	
Kumar et al., 2022		Commercial instruments	Linear density of fabric	
Wang et al., 2017		Thermal manikin	Thickness of fabric	
Wang et al., 2012		Thermal manikin	Body segments	
Wang et al., 2016	Investigate the factors related to human	Thermal manikin	Sweating set rate	
Fan et al., 2008	Totaled to Haman	Thermal manikin	Motions of human	
Preet et al., 2018	Study the effect of	Commercial instruments	Sweat/water	
Preet et al., 2023	sweat components	Commercial instruments	Lactate concentration	
Wang et al., 2012		Thermal manikin	Wind speed	
Hu et al., 2016	Explore the influence of wind conditions	Thermal manikin	Wind direction	
Cui et al., 2016	wind conditions	Thermal manikin	Wind speed	

Table 1: Investigation on thermal insulation (I_t) and evaporative resistance ($R_{\rm et}$) of fabric.

h between fabrics and the air flow. Asawo et al. (2023)studied the impact of air permeability and wind speed on thermal insulation and Nusselt number. Although they compared the thermal properties of different fabrics, the effect of fabric tightness wasn't considered. The fabrics used in cycling suits typically exhibit high elasticity, resulting in notable changes in surface structure when subjected to stretching (Li et al., 2025). Researchers already know that such surface structural variation can affect the flow and aerodynamic drag (Zheng et al., 2021; Zheng et al., 2023); it is believed that the change in flow state can also affect heat transfer performance of fabric (Cai et al., 2024). Such an effect is not considered in the conventional thermal characterization of fabrics.

On the other hand, current literature lacks systematic experimental measurements of the local convective heat transfer coefficient. Human limbs can be approximated as cylindrical geometries, where fabrics experience highly non-uniform flow and thermal conditions along different circumferential angles (Θ) at high wind speed (Cai et al., 2025). Relying solely on overall heat transfer coefficients is insufficient to accurately estimate thermoregulatory behavior. Although some studies (Sobera et al., 2003; Gibson et al., 2009) employed CFD simulations by simplifying fabrics as porous materials to estimate local Nusselt number, as shown in Figure 1, such models fail to capture the detailed structural features of actual fabrics and provide limited practical guidance.

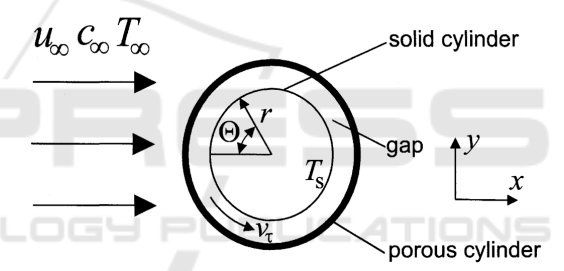


Figure 1: Physical model of limb-air gap-fabric-air flow system (Gibson et al., 2009).

In this study, the effects of stretch ratio and wind speed on the thermal insulation and convective heat transfer coefficient of fabrics were systematically investigated. Local measurements were conducted to elucidate the detailed heat transfer mechanisms, while global values were analyzed to enable direct comparison between the two tested fabrics.

2 METHODOLOGY

2.1 Wind Tunnel Facility

The experiment was conducted using an open-jet wind tunnel in the Aerodynamics and Acoustics Facility at The Hong Kong University of Science and Technology. The wind tunnel has a test section area of 0.6×1.35 m². The flow speed can be adjusted between 0 and 36 km/h.

2.2 Sample Characteristics

In this work, two types of fabrics were selected for investigation (named Fabric A and Fabric B, respectively). The fabrics' pattern, 3D profile, and global surface roughness (*Sa*) were measured by a 3D optical profilometer (VR-6000, KEYENCE, Osaka, Japan), as shown in Table 2. The *Sa* represents the average of the absolute values of surface height deviations from the mean plane over a specified area:

$$Sa = \frac{1}{A} \iint |z(x, y)| dxdy \tag{1}$$

To investigate the thermal performance of sportswear under varying levels of tightness, this study adopts the stretch ratio (SR) as a quantitative measure and examines the variations of the convective heat transfer coefficient h and thermal insulation I_t with respect to SR. The stretch ratio of fabric is defined as follows (Li et al., 2025):

$$SR = \frac{P}{P_0} \tag{2}$$

where P_0 is the original perimeter of fabric, and P is the perimeter of fabric after covering on the cylinder. Obviously, the larger the SR is, the tighter the sportswears are.

The lateral orientation corresponds to the direction orthogonal to the longitudinal grooves. To ensure consistency across measurements, fabric samples were mounted onto the cylindrical surface such that the grooves aligned with the cylinder's axis and remained perpendicular to the airflow. The two cut edges of each fabric piece were stitched together, with the seam positioned at the rear of the cylinder to minimize its impact on the surrounding flow field.

2.3 Experimental System

The system is composed of four primary components: the test section, thermal control system, and data acquisition system, as shown in Figure 2. Some detailed information about instruments and components are listed in Table 3.

2.3.1 Test Section

This section is a cylinder made by resin. Its outer surface can be covered with various fabrics, emulating garments worn on human arms and thighs. The inner surface of the cylinder is equipped with thermocouple slots and water outlets. As illustrated in Figure 3, the T-type thermocouples are installed at 10° intervals to enable the measurement of temperature distribution as a function of angular position (θ).

Fabric A B

Covered on cylinder

Pattern

3D profile

Sa (μm)

114

76

Table 2: Samples' characteristics.

Item	Model	Applicable range	Accuracy	Resolution
Thermocouple	T-type thermocouple	-40 − 125°C	± 0.5°C	_
Infrared camera	FLIR-E5 Pro	-20 − 400°C	± 2%*reading	0.1℃
Power meter	NAPUI-PM9817	0.01 mA - 20 A	± 0.2%	0.001 mW
Temperature regulator	ANTHONE	-10 − 60°C	± 0.2%	0.1°C
Data acquisition	HIOKI-LR8450	-10 − 50°C	-	0.01°C
Optical profilometer	KEYENCE-VR 6000	-15 − 30°C	0.4 μm	0.1 μm

Table 3: Detailed information of the instruments and components used in this work.

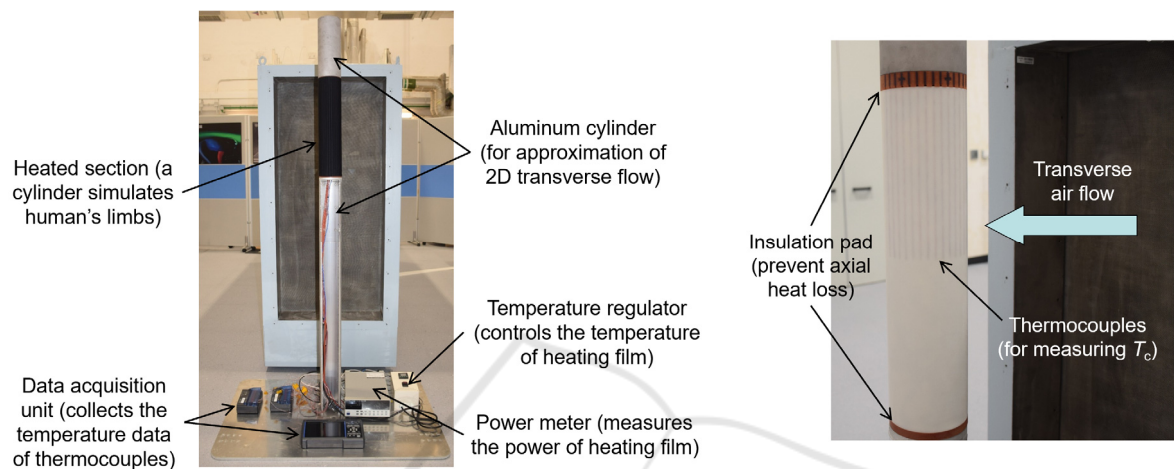


Figure 2: Illustration of experimental system.

2.3.2 Thermal Control System

This system simulates the metabolic heat production of the human body. A heating film adhered to the inner surface of cylinder maintains at a certain temperature, which is controlled by the temperature regulator (ANTHONE, Xiamen, China). The power of heating film is measured by a power meter (NAPUI-PM9817, Dongguan, China). With thermal insulation plates covering both the top and bottom of the cylinder, we assume the heat solely dissipates through the lateral surface of cylinder. This configuration not only aligns with the actual situation of human limbs but also facilitates temperature measurement.

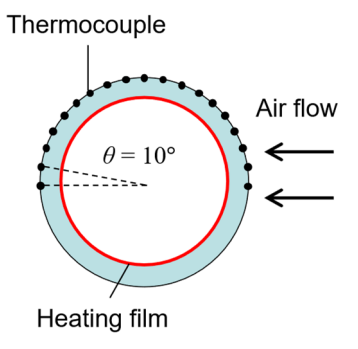


Figure 3: Thermocouples distribution on the cylinder.

2.3.3 Data Acquisition System

It records the temperature and humidity data. The surface and ambient air temperatures are measured using thermocouples, while the temperature of the fabrics' outer surface is measured via an infrared camera (FLIR-E5 Pro, America), as shown in Figure 4. A humidity sensor is used to measure the ambient humidity.



Figure 4: Average temperature at $\theta = 90^{\circ}$.

2.4 Formulation

Under the steady-state condition, the power generated by the heating film H_0 equals to the heat flux conducted from the outer surface of cylinder to fabric's outer surface (H_{cond}). Then the heat flux will dissipate into the environment via two modes: heat convection (H_{conv}) and thermal radiation (H_{rad}). Energy balance of fabric is shown in Figure 5.

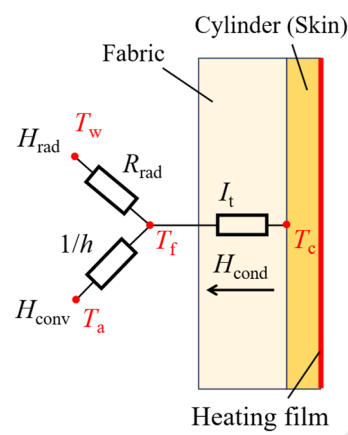


Figure 5: Energy balance of fabric

The energy balance relationship can be expressed as follows:

$$H_0 = H_{\text{cond}} = H_{\text{conv}} + H_{\text{rad}} \tag{3}$$

where H_{cond} , H_{conv} , and H_{rad} represent the steady heat flux through heat conduction, heat convection, and thermal radiation. In view of the ratio of fabric thickness to the curvature, heat conduction within the fabric can be approximated as one-dimensional planar conduction. The corresponding formula is given by:

$$H_{\rm cond} = \frac{A_{\rm f} \cdot (T_{\rm c} - T_{\rm f})}{I_{\rm t}} \tag{4}$$

where $I_{\rm t}$ is the thermal insulation of fabric. $T_{\rm c}$ and $T_{\rm f}$ represent temperature of cylinder outer surface and fabric outer surface, respectively. $A_{\rm f}$ represents the surface area of fabric. The heat convection and thermal radiation can be calculated as:

$$H_{\rm conv} = hA_{\rm f}(T_{\rm f} - T_{\rm a}) \tag{5}$$

$$H_{\rm rad} = A_{\rm f} \varepsilon \sigma (T_{\rm f}^4 - T_{\rm w}^4) \tag{6}$$

where h, T_a , T_w , ε , and σ represent convective heat transfer coefficient, air temperature, wall temperature (for radiant heat exchange), emissivity of fabric, and Stefan-Boltzmann constant. In this work, the local and global values of I_t and h can be calculated combining equations (3) to (6). For local calculation,

 $T_{\rm c}$ and $T_{\rm f}$ are obtained from line-integrated values at the corresponding θ . For global calculations, $T_{\rm c}$ and $T_{\rm f}$ are determined by averaging the values across all θ angles.

3 RESULTS AND DISCUSSION

3.1 Bare Cylinder Test

For verification, the convective heat transfer coefficient h of the bare cylinder is measured under both natural and forced convection conditions ($U_0 = 2, 4, 6, 8 \text{ m/s}$). The results are compared with the semi-empirical models to validate the accuracy of our method. For natural convection, we used the correlation recommended by Churchill et al. for comparison (Churchill & Chu, 1975):

$$Nu = \left\{ 0.825 + \frac{0.387 \cdot Ra^{1/6}}{\left[1 + \left(\frac{0.492}{Pr}\right)^{9/16}\right]^{8/27}} \right\}^{2}$$
 (7)

For forced convection, the correlation developed by Hilpert was selected (Hilpert, 1933):

$$Nu = C \cdot Re^m \cdot Pr^{\frac{1}{3}} \tag{8}$$

where C = 0.193 and m = 0.618 when 4000 < Re <40000; C = 0.027 and m = 0.805 when 40000 < Re <400000. As shown in Figure 6(a), the h measured in this work is $2.45 \text{ W/(m}^2\text{K})$ under natural convection, only 1.92% lower than that of Churchill's correlation. Error bars represent the standard deviation from the mean of three independent measurements. Although the deviation increases with airflow velocity, it remains within an acceptable range. Thus, our experimental system provides a reliable and accurate approach for evaluating the thermal performance of fabrics. Furthermore, we studied the local h at different θ on the cylinder, as shown in Figure 6(b). Our results exhibit good consistency with the previous experimental data (Bergman et al., 2006). They pointed out that when $Re = 10^4$, the flow separation occurs at $\theta \approx 90^{\circ}$.

3.2 Effect of Stretch Ratio on Fabrics' Thermal Performance

In this section, the wind speed was fixed at 8 m/s, and the thermal insulation and convective heat transfer coefficient were measured for two fabrics under different stretch ratios (SR = 1.1, 1.4, 1.7, and 2.0).

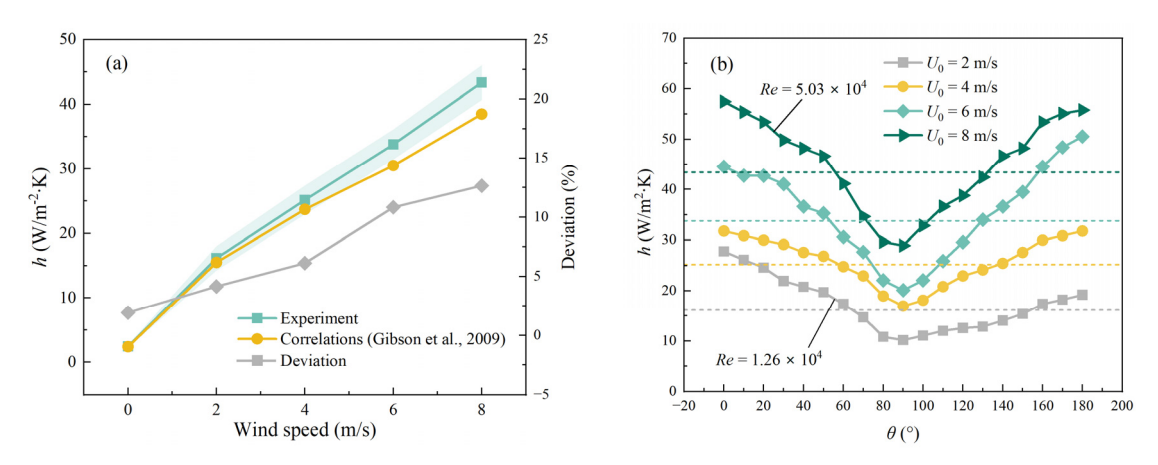


Figure 6: (a) Average and (b) local convective heat transfer coefficient for a bare cylinder.

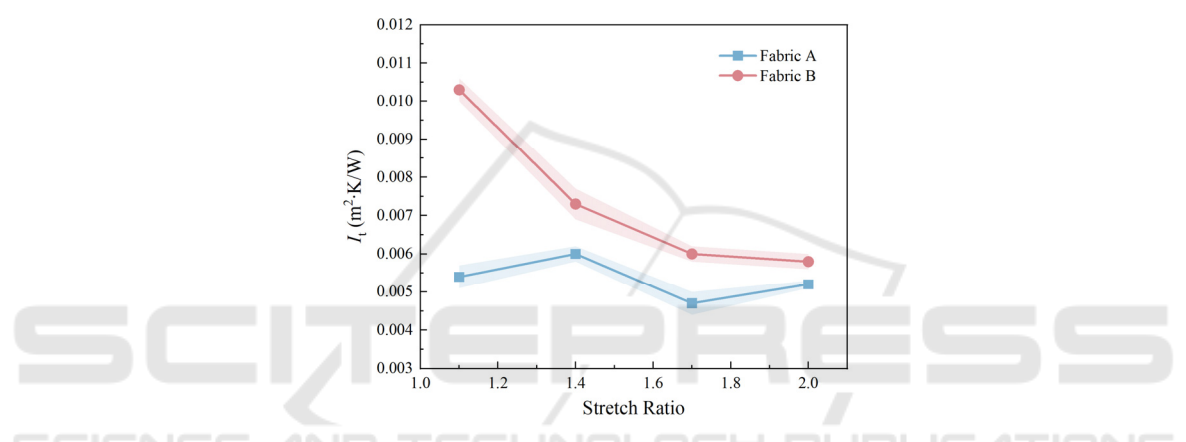


Figure 7: Comparison of fabrics' thermal insulation at different stretch ratio at 8 m/s.

As shown in Figure 7, the thermal insulation of Fabric A fluctuated between 0.0047 and 0.006 m²·K/W with no clear variation tendency. In contrast, the thermal insulation of Fabric B decreased monotonically from 0.0103 to 0.0058 m²·K/W with increasing SR. At all tested SR values, the thermal insulation of Fabric A remained lower than that of Fabric B.

Subsequently, the local thermal insulation at different θ was investigated, as illustrated in Figure 8. Both fabrics exhibited a maximum thermal insulation at $\theta=120^\circ$, and a minimum at $\theta=0^\circ$ or 180° . At $\theta=0^\circ$, which corresponds to the front stagnation point, the incoming airflow impinges directly on the surface and enhances the interfibrous heat convection, thereby reducing thermal insulation. A similar effect occurs at $\theta=180^\circ$ is due to the flow reattachment and turbulence in the wake region. In contrast, $\theta=120^\circ$ typically lies within or just beyond the flow separation zone, where the local flow velocity near the surface is minimal due to boundary layer detachment. This leads to weakened convective heat transfer and hence a local maximum in thermal insulation.

Notice that for Fabric B, the effect of increasing SR on the thermal insulation's reduction diminished when the fabric is very tight. As shown in Figure 8(b), the curves corresponding to SR = 1.7 and 2.0 were nearly identical, indicating a saturation effect. This phenomenon can be explained as follows: thermal insulation is governed by both heat conduction through the fibers and convective heat transfer between the interfibrous air and the fiber surfaces. As the stretch ratio increases, the fabric becomes thinner, which reduces its thermal conduction resistance. Simultaneously, the compression of the fabric decreases the volume fraction of interfibrous air, thereby suppressing the internal convection. Beyond a certain SR (e.g., 1.7), further stretching induces minimal changes in both thickness and internal air content, leading to a stabilized thermal insulation performance. However, the thermal insulation of Fabric A does not stabilize with the increasing SR. The underlying physical mechanism will be explored in future studies.

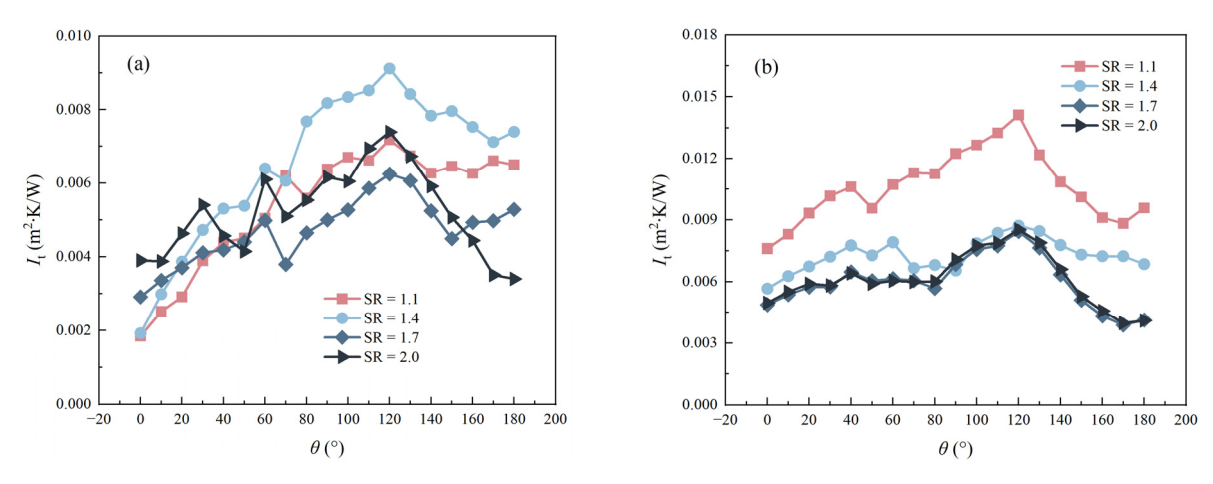


Figure 8: Local value of thermal insulation for (a) Fabric A and (b) Fabric B at different stretch ratio at 8 m/s.

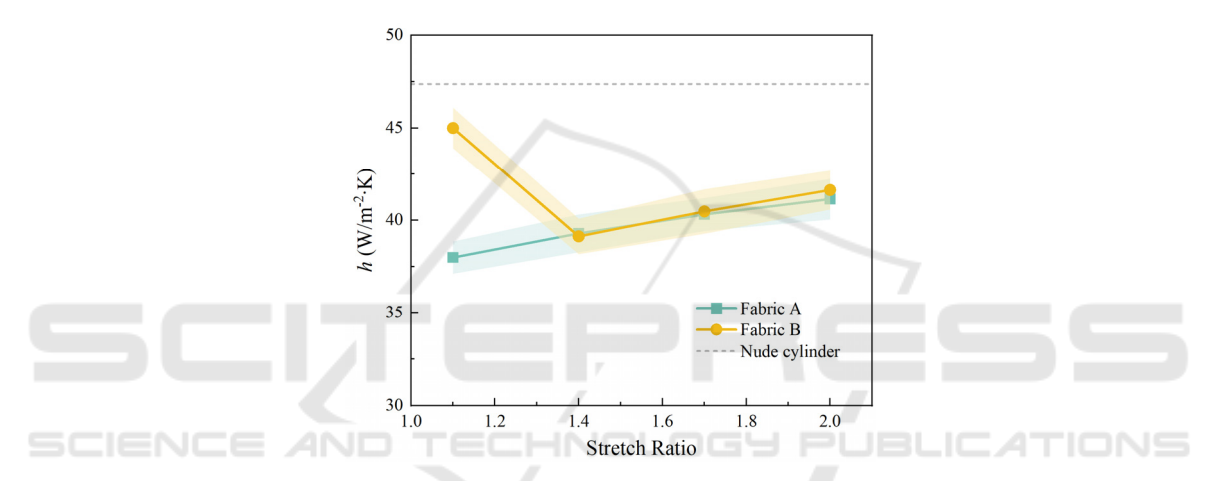


Figure 9: Comparison of convective heat transfer coefficient at different stretch ratio at 8 m/s.

SR also influences the convective heat transfer coefficient of fabric surface. As shown in Figure 9, the convective heat transfer coefficient of Fabric A increases monotonically with SR, with an overall rise of 8.3% from SR = 1.1 to 2.0. In contrast, although Fabric B exhibits a similar increasing trend from SR = 1.4 to 2.0 and shows comparable values to Fabric A, a significant decrease of 13% is observed when SR increases from 1.1 to 1.4.

Local analysis reveals the primary cause of the variations in global value of h. As shown in Figure 10(a), the influence of SR on the convective heat transfer coefficient of Fabric A is mainly concentrated within the range of $\theta = 0^{\circ}-80^{\circ}$, while the region from $80^{\circ}-180^{\circ}$ remains almost unaffected. A similar trend can be observed for Fabric B; however, at SR = 1.1, its local h in the range of $80^{\circ}-180^{\circ}$ are significantly higher than those at other SR values, which accounts for the noticeably higher global h value. Additionally, it is noted that most curves in Figure 10 exhibit a minimum at $\theta = 80^{\circ}$, which is

different from the bare cylinder case where the minimum occurs at $\theta = 90^{\circ}$. It suggests that fabric structure can influence the separation position.

3.3 Effect of Airflow Velocity on Fabrics' Thermal Performance

In this section, SR is fixed at 1.4 to investigate the thermal insulation and convective heat transfer coefficient under varying airflow velocities ($U_0 = 2$, 4, 6, 8 m/s). As shown in Figure 11(a), the thermal insulation of both fabrics decreases with an increasing airflow velocity. This is because, although airflow does not affect the intrinsic thermal conductivity of the fabric, the overall thermal insulation is governed by both heat conduction through the fibers and heat convection of the interfibrous air. Higher airflow enhances inter-fiber convection, thereby reducing the thermal insulation. Additionally, Figure 11(a) shows that Fabric A exhibits lower thermal insulation than

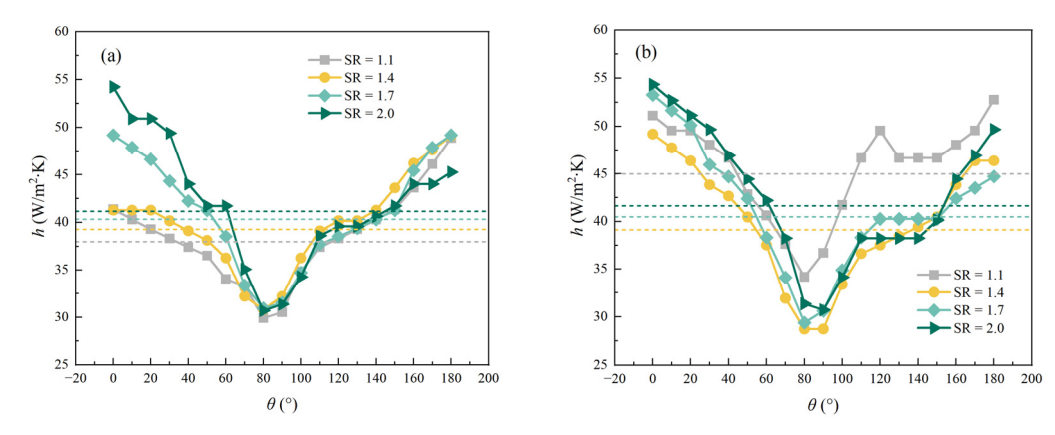


Figure 10: Local convective heat transfer coefficient for (a) Fabric A and (b) Fabric B at different stretch ratio at 8 m/s.

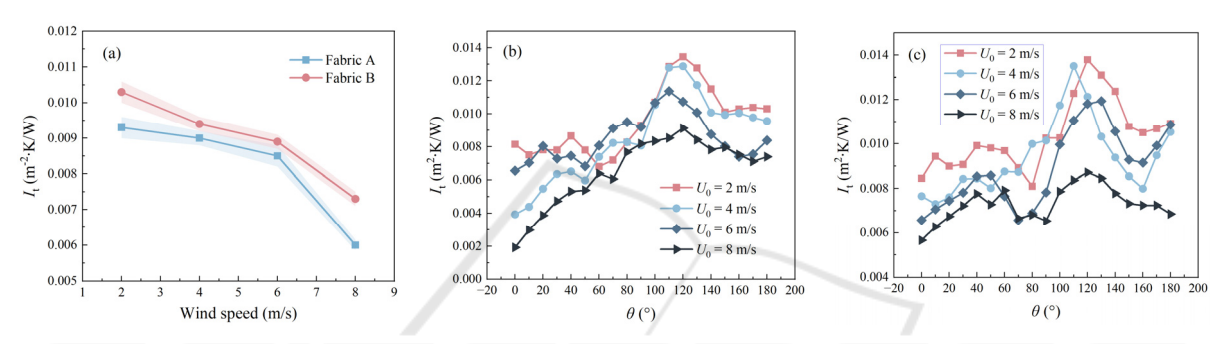


Figure 11: Relationship between thermal insulation and wind speed for fabrics A and B (SR = 1.4). (a) Global values comparison; (b) local value of Fabric A; (c) local value of Fabric B.

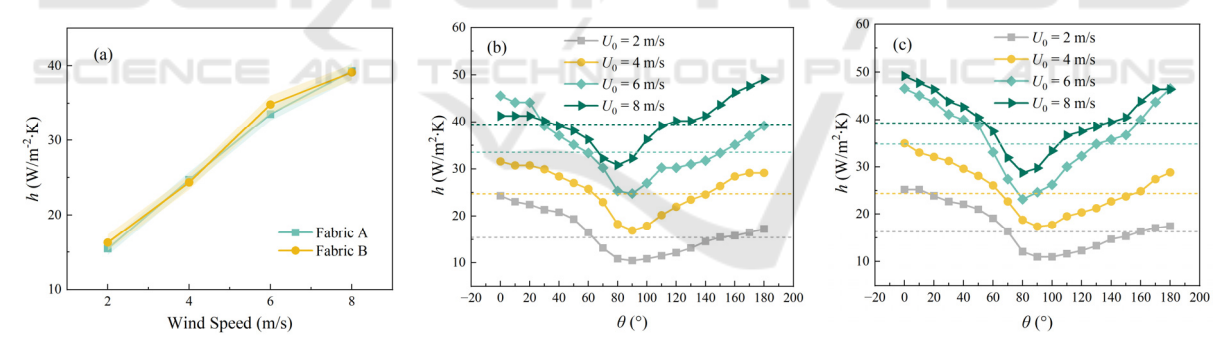


Figure 12: Relationship between convective heat transfer coefficient and wind speed for fabrics A and B (SR = 1.4). (a) Global values comparison; (b) local value of Fabric A; (c) local value of Fabric B.

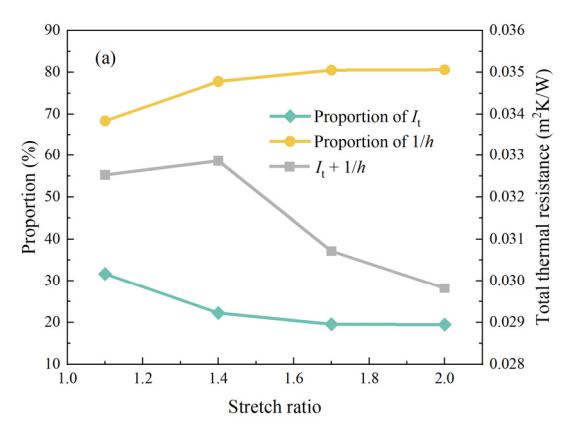
Fabric B throughout all the tested velocities. Figure 11(b) and (c) present the local distributions of thermal insulation, from which a similar conclusion to that in Section 3.2 can be drawn: the local maximum occurs near $\theta = 120^{\circ}$.

Figure 12 shows that the convection heat transfer performance of the two fabrics is nearly identical across all airflow velocities. Figure 12(b) and (c) indicate that within the range of 2–8 m/s, both fabrics maintain a laminar boundary layer, with clear evidence of flow separation. Notably, at lower airflow velocities (below 4 m/s), the separation point appears

near $\theta = 90^{\circ}$, while at higher velocities, it shifts forward to approximately $\theta = 80^{\circ}$. This phenomenon is consistent with the previous results (Bergman, 2006).

3.4 Proportion of Different Thermal Resistances

This study focuses on heat conduction through the fabric and convective heat transfer at its surface. Therefore, radiative heat transfer is neglected in the



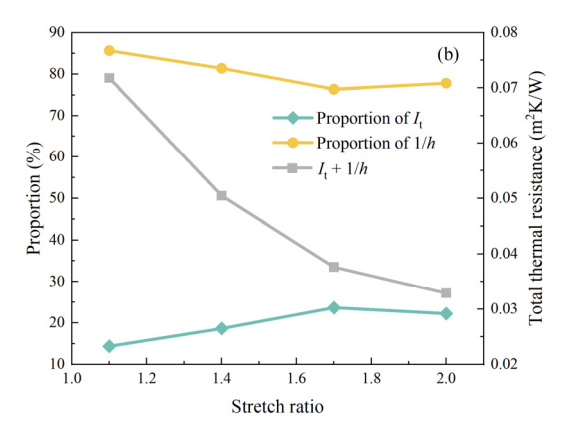


Figure 13: Total thermal resistance and the proportions of thermal insulation and convective thermal resistance as a function of (a) stretch ratio and (b) wind speed.

current analysis. The thermal insulation and convective thermal resistance (1/h) are in series to obtain the total thermal resistance:

$$R_{\text{tot}} = I_{\text{t}} + \frac{1}{h} \tag{9}$$

Taking Fabric B as an example, we examine how the total thermal resistance varies with SR and wind speed, as well as the corresponding changes in the proportion of each thermal resistance. As shown in Figure 13(a), the total thermal resistance of Fabric B tends to decrease with increasing SR. Meanwhile, the percentage of convective thermal resistance increases monotonically from 68% to 80%. Figure 13(b) shows that although the proportion of convective resistance slightly decreases with increasing wind speed, it consistently accounts for more than 78% of the total thermal resistance. These results indicate that within the studied range ($U_0 = 2 - 8 \text{ m/s}$, SR = 1.1 - 2.0), enhancing convective heat transfer is a more effective strategy for improving Fabric B's overall thermal transfer performance of the fabric.

4 CONCLUSIONS

A thermal cylinder platform fixed in the wind tunnel was developed to evaluate the heat transfer performance of sportswear fabrics under varying SR and wind speeds. The key findings are summarized as follows:

The I_t of Fabric B decreased with increasing SR, while Fabric A showed no clear trend. An increase in SR generally enhanced the h for both fabrics, although Fabric B experienced a notable drop in h from SR = 1.1 to 1.4.

Higher wind speeds led to the reduction in I_t and increase in h for both fabrics. Across all wind speeds tested, Fabric A consistently exhibited lower global I_t than Fabric B, while the global h of both fabrics remained nearly identical.

Both fabrics exhibited the maximum I_t at $\theta = 120^\circ$ and minimum values at $\theta = 0^\circ$ or 180°. With increasing wind speed, the flow separation point shifted toward the position with lower θ .

ACKNOWLEDGEMENTS

This work is partially supported by the Hong Kong Innovation and Technology Commission (No. ITS/101/23FP). The study was conducted in the Aerodynamics Acoustics & Noise Control Technology Centre (aantc.ust.hk).

REFERENCES

ASTM International. (2016). Standard test method for measuring the evaporative resistance of clothing using a sweating manikin (ASTM F2370-16). West Conshohocken, PA: ASTM International.

ASTM International. (2022). Standard test method for measuring the thermal insulation of clothing using a heated manikin (ASTM F1291–22). West Conshohocken, PA: ASTM International.

Bergman, T. L., Lavine, A. S., Incropera, F. P., et al. (2006). Fundamentals of heat and mass transfer (7th ed.). Wiley.

Cai, X. Y., Li, H. Z., Ma, T., et al. (2024). Size effect on thermal transport performance of inserted Cu/Cu₃Sn bilayer. *International Journal of Heat and Mass Transfer*, 218, 124784. https://doi.org/10.1016/j.ijheatmasstrans fer.2023.124784.

Cai, X. Y., Li, H. Z., Zhang, J. Q., et al. (2025). Mechanism of interfacial thermal resistance variation in

- diamond/Cu/CNT tri-layer during thermal cycles. *International Journal of Thermal Sciences*, 207C, 109380. https://doi.org/10.1016/j.ijthermalsci.2024.109380
- Churchill, S. W., & Chu, H. H. S. (1975). Correlating equations for laminar and turbulent free convection from a horizontal cylinder. *International Journal of Heat and Mass Transfer*, 18, 1323–1329. https://doi.org/10.1016/0 017-9310(75)90222-7.
- Cui, Z. Y., Fan, J. T., & Wu, Y. S. (2016). A comparative study on the effects of air gap wind and walking motion on the thermal properties of Arabian Thawbs and Chinese Cheongsams. *Ergonomics*, *59*(8), 999–1008. https://doi.org/10.1080/00140139.2015.1111428.
- Domenico, I. D., Hoffmann, S. M., & Collins, P. K. (2022). The role of sports clothing in thermoregulation, comfort, and performance during exercise in the heat: A narrative review. *Sports Medicine Open, 8*, 58. https://doi.org/10.1186/s40798-022-00449-4.
- Douzi, W., Dupuy, O., Theurot, D., et al. (2020). Percooling (using cooling systems during physical exercise) enhances physical and cognitive performance in hot environments: A narrative review. *International Journal of Environmental Research and Public Health*, 17, 1031. https://doi.org/10.3390/ijerph17031031.
- Fan, J. T., & Tsang, H. W. K. (2008). Effect of clothing thermal properties on the thermal comfort sensation during active sports. *Textile Research Journal*, 78(2), 111–118. https://doi.org/10.1177/0040517508080046.
- Gibson, P. (2009). Modeling heat and mass transfer from fabric-covered cylinders. *Journal of Engineered Fibers and Fabrics*, 4(1), 1–8. https://doi.org/10.1177/1558925 00900400102.
- Hilpert, R. (1933). Heat transfer from cylinders. *Ingenieurwes*, 4, 215.
- Hu, S. R., Zhao, M. M., & Li, J. (2016). Effects of wind direction on sportswear thermal insulation with various ease allowance. *International Journal of Clothing Science and Technology*, 28(4), 492–502. https://doi.org/10.1108/IJCST-11-2015-0126.
- Kumar, C. B. S., & Kumar, B. S. (2022). Study on thermal comfort properties of Eri silk knitted fabrics for sportswear application. *Journal of Natural Fibers*, 19(14), 9052–9063. https://doi.org/10.1080/15440478.2 021.1982110.
- Kumar, D. V., & Raja, D. (2021). Study of thermal comfort properties on socks made from recycled polyester/virgin cotton and its blends. *Fibers and Polymers*, 22(3), 841– 846. https://doi.org/10.1007/s12221-021-0471-6.
- Li, X. R., Mao, J. Q. and Zhou, P. (2025). Aerodynamic and Acoustic Evaluation of a Cylinder Covered by Stretched Grooved Fabric. AIAA Journal, https://doi.org/10.25 14/1.J065006.
- Lu, Y. H., Wang, F. M., Peng, H., et al. (2016). Effect of sweating set rate on clothing real evaporative resistance determined on a sweating thermal manikin in a so-called isothermal condition (*T*_{manikin} = *T*_a = *T*_r). *International Journal of Biometeorology, 60,* 481–488. http://dx.doi.org/10.1007/s00484-015-1029-3.
- Mukhopadhyay, A., Preet, A., & Midha, V. (2018). Moisture transmission behavior of individual component and multi-layered fabric with sweat and pure water. *The*

- Journal of The Textile Institute, 109(3), 383–392. https://doi.org/10.1080/00405000.2017.1348435.
- Noshrodkoli, M. R., Mousazadegana, F., Gharehaghaji, A., et al. (2024). How porosity of the middle layer can affect the comfort properties of multi-layer sportswear. *The Journal of The Textile Institute*. https://doi.org/10.1080/00405000.2024.2351668.
- Özkan, E. T., Kaplangiray, B., Şekir, U., et al. (2023). Investigation of the thermal comfort of the sportswear by standing thermal manikin and thermal imaging techniques. *Journal of Engineered Fibers and Fabrics*, 18, 1–12. https://doi.org/10.1177/15589250231180248.
- Preet, A., Mukhopadhyay, A., & Midha, V. K. (2023). Impact of varying lactate concentration in sweat on thermophysiological comfort of multi-layered ensembles. *International Journal of Clothing Science and Technology*, 35(2), 266–276. https://doi.org/10.1108/ IJCST-12-2021-0176.
- Reilly, T., Drust, B., & Gregson, W. (2006). Thermoregulation in elite athletes. *Current Opinion in Clinical Nutrition and Metabolic Care*, 9(6), 666–671. https://doi.org/10.1097/01.mco.0000247475.95026.a5.
- Saeed, M. A., Safdar, F., Basit, A., et al. (2022). Development of thermally comfortable clothing for hot and humid environment. *Journal of Natural Fibers*, 19(14), 7674–7686. https://doi.org/10.1080/15440478.2 021.1958404.
- Sobera, M. P., Kleijn, C. R., & Van den Akker, H. E. A. (2003). Convective heat and mass transfer to a cylinder sheathed by a porous layer. *AIChE Journal*, 49(12), 3018–3028. https://doi.org/10.1002/aic.690491204.
- Tamsaki, A., David, T., & David, S. (2023). Measuring convective heat transfer coefficients and thermal resistance for protective fabrics using a heated cylinder in a wind tunnel. *The Journal of The Textile Institute*, 114(12), 1909–1917. https://doi.org/10.1080/004050 00.2022.2150956.
- Tesinova, P., & Atalie, D. (2022). Thermal comfort properties of sport fabrics with dependency on structure parameters and maintenance. *Fibers and Polymers*, 23(4), 1150–1160. https://doi.org/10.1007/s12221-022-4160.x
- Wang, F. M., Ferraro, S., Lin, L. Y., et al. (2012). Localised boundary air layer and clothing evaporative resistances for individual body segments. *Ergonomics*, *55*(7), 799–812. https://doi.org/10.1080/00140139.2012.668948.
- Wang, F. M., Lai, D. D., Shi, W., et al. (2017). Effects of fabric thickness and material on apparent 'wet' conductive thermal resistance of knitted fabric 'skin' on sweating manikins. *Journal of Thermal Biology*, 70, 69– 76. http://dx.doi.org/10.1016/j.jtherbio.2017.03.004.
- Zheng, C. T., Zhou, P., Zhong, S. Y., et al. (2021). An experimental investigation of drag and noise reduction from a circular cylinder using longitudinal grooves. *Physics of Fluids*, 33, 115110. https://doi.org/10.1063/ 5.0070959.
- Zheng, C. T., Zhou, P., Zhong, S. Y., et al. (2023). On the cylinder noise and drag reductions in different Reynolds number ranges using surface pattern fabrics. *Physics of Fluids*, 35, 035111. https://doi.org/10.1063/5.0138074.